JOURNAL OF GUIDANCE, CONTROL, AND DYNAMICS
Vol. 19, No. 6, November–December 1996

Position Tracking Control of a Smart Flexible Structure Featuring a Piezofilm Actuator

Seung-Bok Choi,* Chae-Cheon Cheong,† and Chul-Hee Lee‡
Inha University, Incheon 402-751, Republic of Korea

A position tracking control of a smart flexible structure with a piezofilm actuator is presented. A governing equation of motion for a smart cantilevered beam is derived via Hamilton's principle, and a reduced-order control model is subsequently obtained through a modal analysis. Uncertain system parameters such as frequency variations are included in the control model. A sliding-mode control theory, which has inherent robustness to system uncertainties, is adopted to design a position tracking controller for the piezofilm actuator. Using the output information from a tip displacement sensor, a full-order observer is constructed to estimate state variables of the control system. Tracking control performances for desired position trajectories represented by sinusoidal and step functions are evaluated by undertaking both simulation and experimental works.

Nomenclature

A_1 = cross-sectional area of the composite beam
A_2 = cross-sectional area of the piezofilm
b = width of the composite beam (or piezofilm)
d_i = magnitude of the disturbance
d_{31} = piezoelectric strain constant
E_1 = elastic modulus of the composite beam
E_2 = elastic modulus of the piezofilm
e = tracking error of the tip displacement
f = external disturbance
g = gradient of the sliding surface
h_1 = thickness of the composite beam
h_2 = thickness of the piezofilm
I_i = generalized mass
I_1 = area moment of inertia of the composite beam
I_2 = area moment of inertia of the piezofilm
k = discontinuity gain of the sliding-mode controller
L = length of the composite beam (or piezofilm)
q_i = generalized modal coordinate
$\mathbf{R}$ = observer matrix
s = sliding surface
t = time variable
T_k = kinetic energy
V = control input voltage
V_p = potential energy
x = spatial variable in the axial direction
x_i = state variable
$\hat{x}_i$ = estimated state variable
y_{dt} = desired tip displacement
y_t = actual tip displacement
β_i = weighting factor of the natural frequency deviation
γ_i = weighting factor of the damping ratio deviation
ε = boundary layer width of saturation function
ζ_i = damping ratio
ρ_1 = density of the composite beam
ρ_2 = density of the piezofilm
Φ_i = mode shape function
ω_i = natural frequency

Received Oct. 20, 1995; revision received June 3, 1996; accepted for publication July 5, 1996.

*Associate Professor, Smart Structures and Systems Laboratory, Department of Mechanical Engineering.

†Professor, Smart Structures and Systems Laboratory, Department of Mechanical Engineering.

‡Graduate Research Assistant, Smart Structures and Systems Laboratory, Department of Mechanical Engineering.

Introduction

RECENTLY, with the aid of advanced technologies in computer and material sciences, advanced lightweight structural systems have been designed for application in various research fields such as robotics, space structures, and manufacturing. In particular, the emergence of the so-called smart materials has accelerated successful development of the advanced structural systems. So far, the smart materials include electrorheological fluids,[1] shape memory alloys,[2] and piezoelectric materials.[3–9] The piezoelectric materials considered in this paper have low power consumption, high power-to-weight ratio, and fast response time compared with other smart materials. As of now, piezoelectric materials are most often employed as sensors or actuators for smart structure applications. These smart structures are employed primarily to control the static and elastodynamic responses of distributed parameter systems operating under variable service conditions.

Research on smart structure systems using piezoelectric materials was first undertaken by Bailey and Hubbard.[3] They proposed simple but effective control algorithms for transient-vibration control, namely constant amplitude controller and constant gain controller. Crawley and de Luis[4] analyzed the stiffness effect of piezoelectric actuators on the elastic properties of the host structures. Baz and Poh[5] worked on the vibration control of the smart structures via a modified independent modal space control by considering the effect of the bonding layer between the piezoelectric material and the host structure. Tzou[6] investigated the piezoelectric effect on the vibration control through a modal shape analysis. Subsequently, Choi et al.[7] proposed an optimal control methodology for suppressing elastodynamic responses of high-speed flexible linkage mechanisms. More recently, Choi[8] improved the vibration controllability of the piezofilm actuator by attenuating an undesirable chattering problem in the settling phase.

As is evident from previous studies, numerous researchers have used piezoelectric materials only to focus on the vibration control of the smart structures. However, it is well known that piezoelectric materials also can be utilized as actuators to drive the flexible smart structures. Hence, using the piezoelectric actuator we can directly devise a small-sized flexible arm.[9] The design requirements for this flexible arm include miniature motion, accurate tracking, fast response, and small energy consumption. Furthermore, we can incorporate the piezoelectric actuator into the flexible structure to design a robot gripper imitating a human finger. This type of flexible gripper is capable of executing motion in applications ranging from space structures to microchip manufacture. In general, the flexible gripper can grip soft and tiny objects with small gripping force. The first step to develop successful flexible robot arms or robot grippers is to obtain accurate position tracking of the flexible smart structures. Accordingly, the control objective in the present study is to use the piezofilm actuator to achieve accurate position tracking of the smart structure.

To date, a few investigators have attempted to study position tracking control of the smart flexible structures. Jiang et al.[9] applied piezoelectric patches as actuators to generate the vibration and employed a proportional-integral derivative controller to achieve position tracking of the smart structures. However, they did not consider the robustness of the control system to external disturbances as well as parameter uncertainties such as natural frequency deviation. The occurrence of these system uncertainties is expected in tracking control of flexible structure systems. Therefore, in position tracking control of the smart flexible structures, it is necessary to use an appropriate control strategy that is robust to the system uncertainties.[10] This study adopts a sliding-mode control theory[11] for robust and accurate position tracking control of a smart flexible structure associated with a piezofilm actuator. The piezofilm, also known as polyvinylidene fluoride (PVDF), is a medium that develops mechanical strain when subjected to an electric field or, alternatively, it develops an electric field when subjected to a mechanical deformation. The piezofilm is very suitable for the application of flexible robot arms or robot grippers because it is flexible, light, and tough.

A dynamic governing equation of a partial differential form for a smart cantilevered beam is derived by applying the Hamilton principle. Upon retaining a finite number of vibration modes, a reduced-order control model is obtained in the state-space representation. Furthermore, model parameter variations on natural frequencies and damping ratios of the flexible structure and external disturbances are included in the control model. A sliding mode controller that inherently possesses properties invariant to the parameter variations during the sliding mode motion is proposed and implemented to achieve accurate tracking of the tip displacement. A full-order observer is also constructed to estimate state variables in the control model by using the information from the tip displacement sensor and the control input voltage. Both computer simulation and experimental works for desired position trajectories such as sinusoidal and step motions are undertaken to demonstrate the effectiveness of the proposed control methodology.

Dynamic Modeling

Consider a smart cantilevered beam that has the uniformly distributed piezofilm actuator bonded on the top surface, as shown in Fig. 1. When control voltage $V(x,t)$ is applied to the piezofilm, the induced strain ε_p in the piezofilm is given by[3]

$$\varepsilon_p(x,t) = V(x,t)(d_{31}/h_2) \tag{1}$$

The force equilibrium condition in the axial direction allows one to determine the longitudinal strain component ε_l as follows:

$$\varepsilon_l = \frac{E_2 h_2}{E_1 h_1 + E_2 h_2} \cdot \varepsilon_p \tag{2}$$

The bending moment M produced from the piezofilm actuator due to the application of voltage $V(x,t)$ can be obtained by considering the above equations and the force equilibrium in the axial direction. This is given by

$$M = E_1 h_1 b \varepsilon_l[(h_2/2) - D] - E_2 h_2 b(\varepsilon_p - \varepsilon_l)[(h_2/2) + h_1 - D] \tag{3}$$

where D is the location of the neutral axis of the structure from the bottom surface and is given by

$$D = \frac{E_1 h_1^2 + E_2 h_2^2 + 2h_1 h_2 E_2}{2(E_1 h_1 + E_2 h_2)} \tag{4}$$

Substituting Eqs. (1), (2), and (4) into Eq. (3) yields

$$\begin{aligned} M &= -d_{31}\left(\frac{h_1 + h_2}{2}\right)\frac{E_1 E_2 h_1 b}{(E_1 h_1 + E_2 h_2)} V(x,t) \\ &= cV(x,t) \end{aligned} \tag{5}$$

The constant c is determined by geometrical and material properties of the composite beam and the piezofilm.

When the Bernoulli–Euler beam theory is applied, the kinetic energy T_k and potential energy V_p of the structure including the piezofilm actuator are expressed as[8]

$$T_k = \frac{1}{2}\int_0^L \left[\frac{\partial y(x,t)}{\partial t}\right]^2 \rho A \, dx \tag{6}$$

$$V_p = \frac{1}{2}\int_0^L \frac{1}{EI}\left[EI\frac{\partial^2 y(x,t)}{\partial x^2} + cV(x,t)\right]^2 dx \tag{7}$$

where $EI (= E_1 I_1 + E_2 I_2)$ is the effective bending stiffness of the smart flexible beam and ρA $(= \rho_1 A_1 + \rho_2 A_2)$ is the mass per length of the beam.

By applying the conservation of energy and the Hamilton principle, the governing equation of motion for transverse vibration $y(x,t)$ and associated boundary conditions are obtained as follows:

$$\frac{\partial^2}{\partial x^2}\left[EI\frac{\partial^2 y(x,t)}{\partial x^2} + cV(x,t)\right] + \rho A\frac{\partial^2 y(x,t)}{\partial t^2} = 0 \tag{8}$$

$$\begin{aligned} & y(x,t)|_{x=0} = 0, \qquad \left.\frac{\partial y(x,t)}{\partial x}\right|_{x=0} = 0 \\ & \left.EI\frac{\partial^2 y(x,t)}{\partial x^2}\right|_{x=L} = -cV(x,t)|_{x=L} \\ & \left.EI\frac{\partial^3 y(x,t)}{\partial x^3}\right|_{x=L} = \left.-c\frac{\partial V(x,t)}{\partial x}\right|_{x=L} \end{aligned} \tag{9}$$

Equations (8) and (9) describe a linear distributed parameter system. This system can be rewritten in modal form for computer simulations and controller synthesis.

By introducing the ith modal coordinate $q_i(t)$ and mode shape $\Phi_i(x)$, the deflection $y(x,t)$ can be expressed as follows:

$$y(x,t) = \sum_{i=1}^{\infty} \Phi_i(x) q_i(t) \tag{10}$$

From the boundary conditions (9), the mode shape $\Phi_i(x)$ can be obtained:

$$\begin{aligned} \Phi_i(x) &= \cosh \beta_i x - \cos \beta_i x \\ &\quad - \frac{\sinh \beta_i L - \sin \beta_i L}{\cosh \beta_i L + \cos \beta_i L}(\sinh \beta_i x - \sin \beta_i x) \end{aligned} \tag{11}$$

Here $\beta_i^4 = \rho A \omega_i^2 / EI$, where ω_i is the ith mode natural frequency.

Substituting the energy equations (6) and (7) into the Lagrange equation and augmenting proportional damping, a decoupled

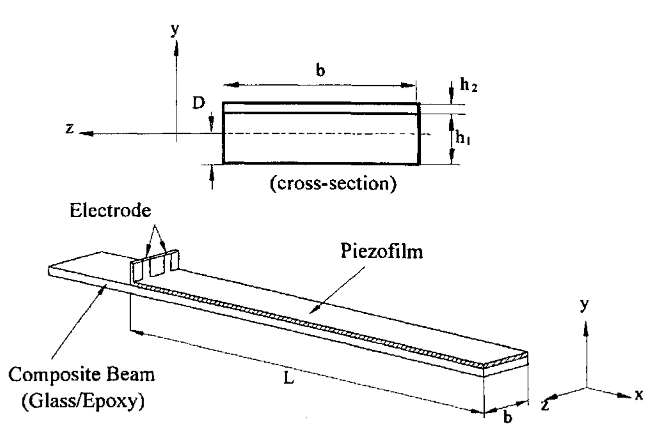

Fig. 1 Schematic diagram of a smart structure beam.

ordinary differential equation for each mode of the proposed smart structure is obtained:

$$\ddot{q}_i + 2\zeta_i\omega_i\dot{q}_i + \omega_i^2 q_i = -\frac{cV(t)}{I_i}\int_0^L \frac{\partial^2\Phi_i}{\partial x^2}\,\mathrm{d}x \tag{12}$$

where ζ_i is the damping ratio of the ith mode and I_i is the generalized mass, given by

$$I_i = \int_0^L \Phi_i^2(x)\rho A\,\mathrm{d}x \tag{13}$$

Controller Design

Upon retaining a finite number of control modes, a reduced dynamic model can be obtained in the state-space representation as follows:

$$\dot{\boldsymbol{x}}(t) = \boldsymbol{A}\boldsymbol{x}(t) + \boldsymbol{B}V(t) + \boldsymbol{D}f(t) \qquad y(t) = \boldsymbol{C}\boldsymbol{x}(t) \tag{14}$$

where

$$\boldsymbol{x} = [q_1 \quad \dot{q}_1 \quad q_2 \quad \dot{q}_2 \quad \cdots \quad q_n \quad \dot{q}_n]^T \tag{15}$$

$$\boldsymbol{A} = \begin{bmatrix} 0 & 1 & & & \\ -\omega_1^2 & -2\zeta_1\omega_1 & & & \\ & & \ddots & & \\ & & & 0 & 1 \\ & & & -\omega_n^2 & -2\zeta_n\omega_n \end{bmatrix}$$

$$\boldsymbol{B} = -c\left[0 \quad \frac{1}{I_1}\int_0^L \frac{\partial^2\Phi_1}{\partial x^2}\,\mathrm{d}x \quad \cdots \quad 0 \quad \frac{1}{I_n}\int_0^L \frac{\partial^2\Phi_n}{\partial x^2}\,\mathrm{d}x\right]^T$$

$$\boldsymbol{C} = [\Phi_1(L) \quad 0 \quad \cdots \quad \Phi_n(L) \quad 0] \tag{16}$$

$$\boldsymbol{D} = [0 \quad d_1 \quad \cdots \quad 0 \quad d_n]^T$$

In Eq. (14), $f(t)$ is an unknown but bounded external disturbance to be expected in system environments and hardware equipment. For example, electrical noise (normally 60 Hz), unexpected airflow, and ground impact may occur in the experimental realization. Note that the output matrix $\boldsymbol{C}$ is related to the tip position (y_t) sensor.

Now, we introduce a tracking error to drive it to 0 for any arbitrary initial condition as follows:

$$\begin{aligned} e(t) &= y_t - y_{\mathrm{dt}} = \sum_{i=1}^n \Phi_i(L)x_i(t) - y_{\mathrm{dt}} \\ \dot{e}(t) &= \dot{y}_t - \dot{y}_{\mathrm{dt}} = \sum_{i=1}^n \Phi_i(L)\dot{x}_i(t) - \dot{y}_{\mathrm{dt}} \end{aligned} \tag{17}$$

Here y_{dt} is the desired trajectory of the tip position that belongs to the set of continuously differentiable functions. The state variables of $x_i(t)$ and $\dot{x}_i(t)$ represent $q_i(t)$ and $\dot{q}_i(t)$, respectively.

The problem now is to design a sliding surface that guarantees stable sliding-mode motion on the surface itself. Because there is only one control input, we construct one sliding surface for the system (14):

$$\begin{aligned} s &= ge(t) + \dot{e}(t) \\ &= g\left[\sum_{i=1}^n \Phi_i(L)x_i(t) - y_{\mathrm{dt}}\right] + \left[\sum_{i=1}^n \Phi_i(L)\dot{x}_i(t) - \dot{y}_{\mathrm{dt}}\right] \end{aligned}$$

$$g > 0 \tag{18}$$

Then the following sliding condition is introduced to guarantee that the state variables of the system during the sliding mode motion are constrained to the sliding surface:

$$s\dot{s} < 0 \tag{19}$$

To find a sliding-mode controller that satisfies this sliding condition, we take the time derivative of the sliding surface defined by Eq. (18):

$$\begin{aligned} \dot{s} &= g\left[\sum_{i=1}^n \Phi_i(L)\dot{x}_i - \dot{y}_{\mathrm{dt}}\right] + \left[\sum_{i=1}^n \Phi_i(L)\ddot{x}_i - \ddot{y}_{\mathrm{dt}}\right] \\ &= g\left[\sum_{i=1}^n \Phi_i(L)\dot{x}_i - \dot{y}_{\mathrm{dt}}\right] + \left\{\sum_{i=1}^n \Phi_i(L) \right. \\ &\quad \left. \times \left[-\omega_i^2 x_i - 2\zeta_i\omega_i\dot{x}_i + d_i f(t)\right] - \ddot{y}_{\mathrm{dt}}\right\} + PV(t) \end{aligned} \tag{20}$$

Here,

$$P = -c\sum_{i=1}^n \frac{\Phi_i(L)}{I_i}\int_0^L \frac{\partial^2\Phi_i}{\partial x^2}\,\mathrm{d}x$$

Then the following sliding-mode controller $V(t)$ satisfies the sliding-mode condition (19):

$$V(t) = -\frac{1}{P}\left\{g\left[\sum_{i=1}^n \Phi_i(L)\dot{x}_i - \dot{y}_{\mathrm{dt}}\right] + \sum_{i=1}^n \Phi_i(L)\left(-\omega_i^2 x_i - 2\zeta_i\omega_i\dot{x}_i\right) - \ddot{y}_{\mathrm{dt}}\right] + k\,\mathrm{sgn}(s)\right\} \tag{21}$$

Here,

$$k > \sum_{i=1}^n \Phi_i(L)d_i|f(t)|$$

We know that, in practice, it is not desirable to use the discontinuous control law (21) because of the chattering. Therefore, we approximate the discontinuous control law by a continuous one inside the boundary layer width (ε).[12,13] To do this, we may replace sgn(s) in Eq. (21) by a saturation function, sat(s), defined as

$$\mathrm{sat}(s) = \begin{cases} s/\varepsilon, & |s| \le \varepsilon \\ \mathrm{sgn}(s), & |s| > \varepsilon \end{cases} \tag{22}$$

The controller (21) is designed for the control system, which does not include the system uncertainties. We construct a robust controller that guarantees stable performance of the system for all possible variations of system parameters by treating the variations as uncertainties. The possible variations of the model parameters such as natural frequencies and damping ratios can occur in practice because of varying tip mass or measurement errors. These variations can be expressed as follows:

$$\begin{aligned} \omega_i &= \omega_{0,i} + \delta\omega_i, & |\delta\omega_i| &\le \beta_i\omega_{0,i} \\ \zeta_i &= \zeta_{0,i} + \delta\zeta_i, & |\delta\zeta_i| &\le \gamma_i\zeta_{0,i} \end{aligned} \tag{23}$$

Here $\omega_{0,i}$ and $\zeta_{0,i}$ are the nominal natural frequency and the damping ratio of the ith mode, respectively. The $\delta\omega_i$ and $\delta\zeta_i$ are corresponding possible deviations due to, for instance, the varying tip mass. Note that the variations of the $\delta\omega_i$ and $\delta\zeta_i$ are bounded by the weighting factors β_i and γ_i, respectively.

Now, substituting Eq. (23) into the system matrix $\boldsymbol{A}$ in Eq. (14) yields the following dynamic model, which divides the system matrix $\boldsymbol{A}$ into the nominal part $\boldsymbol{A}_0$ and uncertain part $\Delta\boldsymbol{A}$:

$$\dot{\boldsymbol{x}}(t) = (\boldsymbol{A}_0 + \Delta\boldsymbol{A})\boldsymbol{x}(t) + \boldsymbol{B}V(t) + \boldsymbol{D}f(t) \qquad y(t) = \boldsymbol{C}\boldsymbol{x}(t) \tag{24}$$

To formulate a sliding-mode controller for the uncertain dynamic model, differentiating the sliding surface (18) with respect to time yields

$$\dot{s} = g\left[\sum_{i=1}^n \Phi_i(L)\dot{x}_i - \dot{y}_{\mathrm{dt}}\right] + \left\{\sum_{i=1}^n \Phi_i(L)[(r_{2i-1} + p_{2i-1})x_i + (r_{2i} + p_{2i})\dot{x}_i + d_i f(t)] - \ddot{y}_{\mathrm{dt}}\right\} + PV(t) \tag{25}$$

Here,

$$r_{2i-1} = -\omega_{0,i}^2, \qquad p_{2i-1} = -\left(2\omega_{0,i}\delta\omega_i + \delta\omega_i^2\right)$$

$$r_{2i} = -2\zeta_{0,i}\omega_{0,i}, \qquad p_{2i} = -2(\omega_{0,i}\delta\zeta_i + \zeta_{0,i}\delta\omega_i + \delta\omega_i\delta\zeta_i)$$

Thus, the following sliding mode controller, which is robust to the parameter variations, is obtained from the sliding mode condition (19):

$$V(t) = -\frac{1}{P}\left\{ g\left[\sum_{i=1}^{n}\Phi_i(L)\dot{x}_i - \dot{y}_{dt}\right] + \left[\sum_{i=1}^{n}\Phi_i(L)(r_{2i-1}x_i + r_{2i}\dot{x}_i) - \ddot{y}_{dt}\right] + \left[k + \sum_{i=1}^{n}|\Phi_i(L)|(|z_{2i-1}x_i| + |z_{2i}\dot{x}_i|)\right]\mathrm{sgn}(s)\right\} \tag{26}$$

Here,

$$z_{2i-1} = -\left(2\omega_{0,i}\beta_i\omega_{0,i} + \beta_i^2\omega_{0,i}^2\right)$$

$$z_{2i} = -2(\gamma_i\zeta_{0,i}\omega_{0,i} + \beta_i\omega_{0,i}\zeta_{0,i} + \gamma_i\beta_i\omega_{0,i}\zeta_{0,i})$$

$$k > \sum_{i=1}^{n}\Phi_i(L)d_i|f(t)|$$

Then, we can show that the uncertain system (24) with the proposed controller (26) satisfies the sliding condition (19) as follows:

$$s\dot{s} = s\left(g\left[\sum_{i=1}^{n}\Phi_i(L)\dot{x}_i - \dot{y}_{dt}\right] + \left\{\sum_{i=1}^{n}\Phi_i(L)[(r_{2i-1} + p_{2i-1})x_i + (r_{2i} + p_{2i})\dot{x}_i + d_i f(t)] - \ddot{y}_{dt}\right\} + PV(t)\right)$$

$$= s\left\{\sum_{i=1}^{n}\Phi_i(L)[p_{2i-1}x_i + p_{2i}\dot{x}_i + d_i f(t)] - \left[k + \sum_{i=1}^{n}|\Phi_i(L)|(|z_{2i-1}x_i| + |z_{2i}\dot{x}_i|)\right]\mathrm{sgn}(s)\right\} < 0 \tag{27}$$

All of the state variables used in the proposed controller (26) are not available from direct measurements. With the knowledge of given matrices $\boldsymbol{A}_0$, $\boldsymbol{B}$, and $\boldsymbol{C}$, we can estimate the state variables by designing an appropriate observer. A full-order observer[14] is designed in this study with the information of the input control voltage and the tip position sensor signal of the smart flexible structure:

$$\dot{\bar{x}}(t) = (\boldsymbol{A}_0 - \boldsymbol{RC})\bar{x}(t) + \boldsymbol{R}y_t + \boldsymbol{B}V(t)$$
$$\boldsymbol{R} = [r_1 \quad r_2 \quad \cdots \quad r_{2n-1} \quad r_{2n}]^T \tag{28}$$

Note that the observer matrix $\boldsymbol{R}$ is to be appropriately determined so that all of the desired eigenvalues of the matrix $[\boldsymbol{A}_0 - \boldsymbol{RC}]$ have negative real parts. Using the estimated state variables, we can implement the sliding-mode controller (26) for the position tracking control.

Note that although the sliding-mode controller (26) may be robust to parameter uncertainties, the robustness of the observer-based sliding-mode controller may not be guaranteed. The robustness to parameter uncertainties can be guaranteed by employing a robust sliding-mode observer.[15]

Results and Discussion

The dimensional and material specifications of the composite beam and the piezofilm used in this study are presented in Table 1. Figure 2 presents a schematic diagram of the experimental apparatus and associated instrumentation. A piezofilm bonded on the upper surface of the composite beam is employed as an actuator to construct a feedback control system. The tip displacement

Table 1 Dimensional and mechanical properties of the composite beam and piezofilm

Young's modulus, GPa	Thickness, mm	Density, kg/m^3	Width, mm	Length, mm
		Composite beam (glass/epoxy)		
6.4	0.5	1865	27.0	170.0
		Piezofilm (PVDF)[a]		
2	0.110	1780	27.0	170.0

[a]Piezoelectric strain constant $d_{31} = 23 \times 10^{-12}$(mV^{-1}).

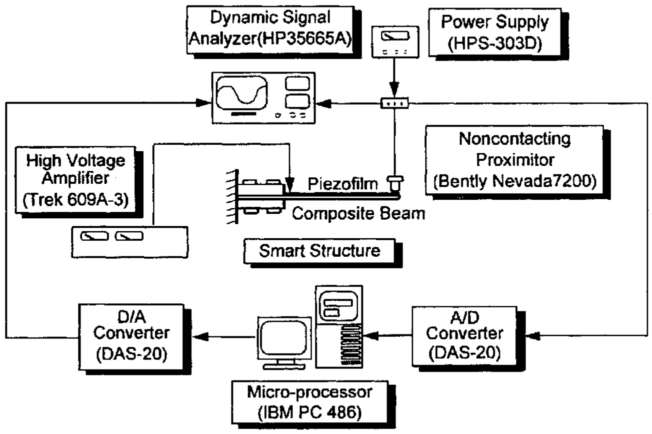

Fig. 2 Experimental apparatus for position tracking control.

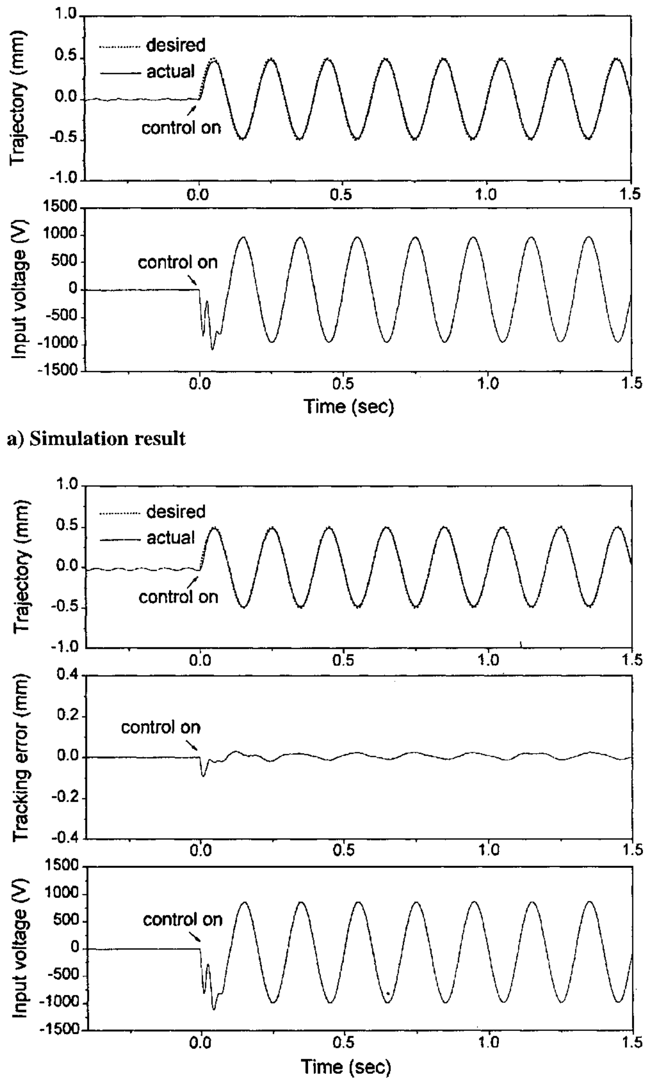

b) Experiment result

Fig. 3 Tracking performance for sinusoidal trajectory.

is monitored by a noncontacting displacement sensor (proximitor) manufactured by Bently Nevade Corporation (Model 7200). The required negative input voltage is supplied from a dc power supply (HPS-303D). The tip displacement is fed back to the microprocessor through the analog/digital converter, which has 12 bits (DAS-20). Depending on the information of the tip displacement and input voltage signal, the full-order observer calculates all of the state variables of the proposed controller. By using the estimated state variables, control input voltage is determined in the microprocessor (IBM personal computer 486) by means of the proposed sliding-mode controller. The sampling rate is chosen by 1000 Hz. The control voltage of the microprocessor is applied to the piezofilm actuator after being amplified via a high-voltage amplifier (Trek 609A-3), which has a gain of 1000. To demonstrate the superior control performance characteristics of the proposed control methodology, a dynamic signal analyzer (HP 35665A) is used to save and analyze the experimental results.

Figure 3 presents tracking control results for the desired position trajectory of sine function used frequently in the tracking demonstration. The first and second flexible modes were considered as the primary modes to be controlled in the implementation. The system model parameters were experimentally obtained as follows: $\omega_1 = 12$ Hz, $\omega_2 = 76.3$ Hz, $\zeta_1 = 0.0072$, and $\zeta_2 = 0.00432$. To demonstrate the robustness to the external disturbance, $d_1 f(t) = 0.1\sin(120\pi t)$ and $d_2 f(t) = 0.005\sin(120\pi t)$ were imposed to both the simulation and the experiment. In the experimental implementation, the source of the disturbance was supplied from the dynamic signal analyzer. The following control parameters such as the sliding surface constant, the boundary layer width, and the discontinuity control gain were employed: $g = 100$, $\varepsilon = 0.3$, and $k = 15$. The desired eigenvalues of the full-order observer were chosen by $-5.0 \pm 75i$, $-5.0 \pm 480i$. For the control results shown in Fig. 3, the sliding-mode controller (21) was implemented. It is observed from the trajectory response that the settling time to the desired trajectory is about 0.1 s, and there exists an error of 0.02 mm in the vicinity of the peak of the desired trajectory. This tracking error is attributed to the fact that the proposed controller includes the saturation function. Note that the error may be reduced by decreasing the value of boundary layer width ε, but the precision control performance may be degraded because of the increment of the chattering in control input voltage. We clearly see that there exists excellent agreement between the simulation and experiment results.

The tracking control results for the desired position of step function with a period of 2 s are presented in Fig. 4. This type of motion is widely required for the actual robot gripper. All of the control parameters for the simulation and the experiment were the same as those in Fig. 3 except for the boundary layer width of $\varepsilon = 0.25$. It is clear from the control results that the piezofilm actuator quickly responds in the presence of the chattering of the control input voltage when the step trajectory is changed from the positive to the negative position every second. It is also shown that the settling time is about 0.2 s for each sudden change of the desired trajectory without overshoot. The settling time may be shortened by increasing the sliding surface constant (g). However, the higher control voltage due to the higher sliding surface constant is required and this may break down the proposed piezofilm. We see that the experimental results agree very well with the simulation results, and this achievement of the tracking control performance featuring fast and accurate responses provides a prominent feasibility of being applied to the precise position control of the flexible robot arms or robot grippers.

In Fig. 5, the tracking results for the sinusoidal desired trajectory of varying frequency are given. The frequency varies from 1 to

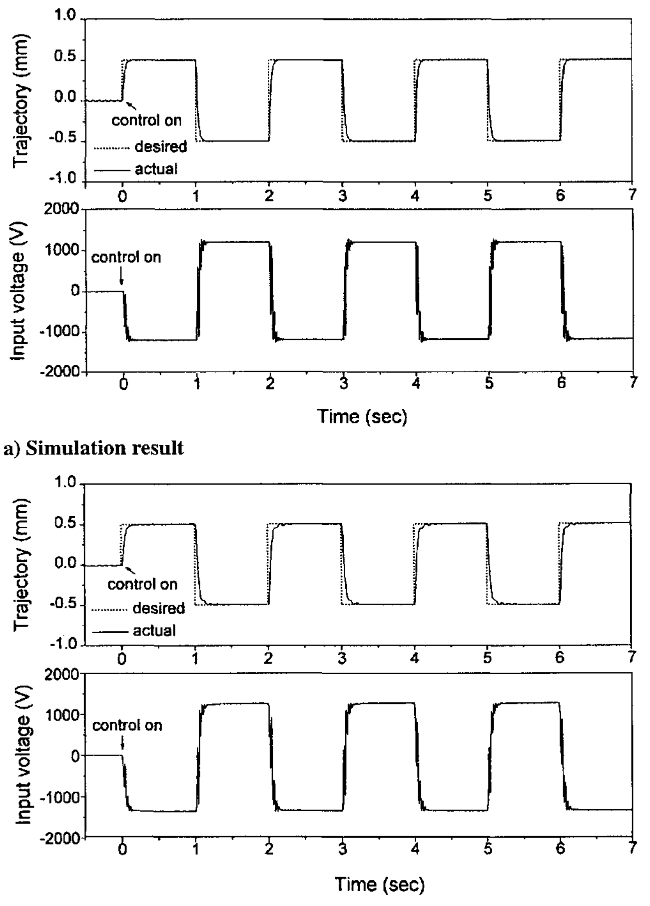

a) Simulation result

b) Experiment result

Fig. 4 Tracking performance for step trajectory.

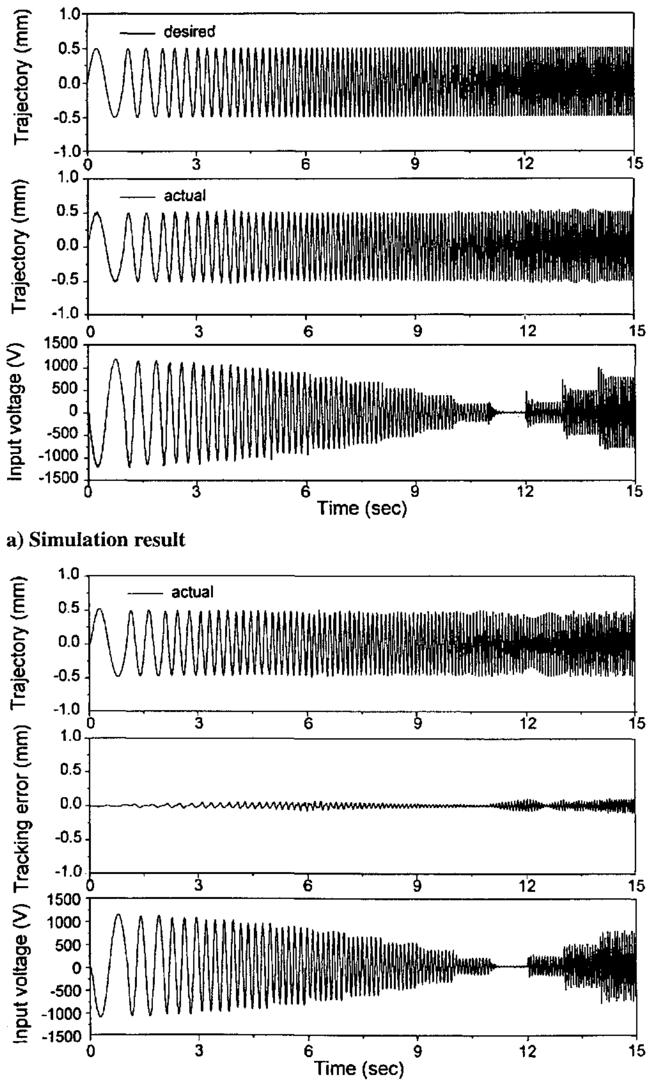

a) Simulation result

b) Experiment result

Fig. 5 Tracking performance for sinusoidal trajectory of varying frequency.

15 Hz. The parameter variations were imposed by using the following weighting factors on the natural frequency and the damping ratio: $\beta_1 = 4\%$ (12 ± 0.48 Hz), $\beta_2 = 1\%$ (76.3 ± 0.763 Hz), $\gamma_1 = 10\%$ (0.0072 ± 0.00072), and $\gamma_2 = 5\%$ (0.00432 ± 0.000216). These parameter variations were augmented to the actual model parameters in the controller design. Therefore, the sliding-mode controller (26) was employed to account for the imposed parameter variations in the simulation and in the experiment. The observer was constructed by choosing desired eigenvalues of $-1.0 \pm 75.4i$ and $-1.0 \pm 479.3i$. It is clear that the position tracking is successfully performed over the chosen frequency range. From the control voltage history, we know that the control voltage required to generate the imposed magnitude of the end displacement decreases as the frequency approaches the first natural frequency (12 Hz) of the system and increases after that. Even though the tracking performance is degraded in the changing phase from the first mode to the second mode, the results are quite self-explanatory and show that we may achieve fast and accurate tracking performance by using the piezofilm actuator.

Conclusions

A position tracking control of a smart flexible structure featuring a piezofilm actuator was presented in this paper. Following a construction of a control system model that contains external disturbance and parameter variations such as frequency deviation, a sliding-mode controller was formulated on the basis of the sliding-mode condition. A full-order observer was designed to estimate state variables, which are necessary for implementation of the controller. The sinusoidal and step trajectories were imposed and tracking performances were evaluated through both computer simulation and experimental realization. Favorable control performances were achieved in terms of tracking accuracy and control robustness. In addition, the agreement between experimental and simulation results is excellent. The results achieved in this study will be used as the basis for constructing flexible robot arms or robot grippers operated by piezoelectric actuators. It is finally remarked that a subsequent task to achieve successful robot grippers is to develop an appropriate compliant control algorithm that accounts for both the position and force control requirements.

Acknowledgments

This work was partially supported by the Korea Science and Engineering Foundation under Contract 951-1008-068-1. This financial support is gratefully acknowledged. The authors also would like to thank one of the reviewers for valuable comments.

References

[1]Choi, S. B., Park, Y. K., and Suh, M. S., "Elastodynamic Characteristics of Hollow Cantilever Beams Containing an Electro-Rheological Fluid: Experimental Results," *AIAA Journal*, Vol. 32, No. 2, 1994, pp. 438–440.

[2]Rogers, C. A., "Active Vibration and Structural Acoustic Control of Shape Memory Alloy Hybrid Composites: Experimental Results," *Journal of the Acoustical Society of America*, Vol. 88, No. 6, 1990, pp. 2803–2811.

[3]Bailey, T., and Hubbard, J. E., Jr., "Distributed Piezoelectric-Polymer Active Vibration Control of a Cantilever Beam," *Journal of Guidance, Control, and Dynamics*, Vol. 8, No. 5, 1985, pp. 605–611.

[4]Crawley, E. F., and de Luis, J., "Use of Piezoelectric Actuators as Elements of Intelligent Structures," *AIAA Journal*, Vol. 25, No. 10, 1987, pp. 1373–1385.

[5]Baz, A., and Poh, S., "Performance of an Active Control System with Piezoelectric Actuators," *Journal of Sound and Vibration*, Vol. 126, No. 2, 1988, pp. 327–343.

[6]Tzou, H. S., "Distributed Modal Identification and Vibration Control of Continua: Theory and Applications," *Journal of Dynamic Systems, Measurement and Control*, Vol. 113, 1991, pp. 494–499.

[7]Choi, S. B., Cheong, C. C., Thompson, B. S., and Gandhi, M. V., "Vibration Control of Flexible Linkage Mechanisms Using Piezoelectric Films," *Mechanism and Machine Theory*, Vol. 29, No. 4, 1994, pp. 535–546.

[8]Choi, S. B., "Alleviation of Chattering in a Flexible Beam Control via Piezofilm Actuator and Sensor," *AIAA Journal*, Vol. 33, No. 3, 1995, pp. 564–567.

[9]Jiang, Z W., Chonan, S., and Tani, J., "Tracking Control of a Miniature Flexible Arm Using Piezoelectric Bimorph Cells," *International Journal of Robotics Research*, Vol. 11, No. 3, 1992, pp. 260–267.

[10]Rao, W. S., Butler, R., and Zhao, W., "Robust Multiobjective Controllers for Smart Structures," *Proceedings of the 5th International Conference on Adaptive Structures* (Sendai, Japan), Technomic, Lancaster, PA, 1995, pp. 163–172.

[11]Utkin, V. I., "Variable Structure Systems with Sliding Modes," *IEEE Transactions on Automatic Control*, Vol. AC-22, No. 2, 1977, pp. 212–222.

[12]Choi, S. B., Park, D. W., and Jayasuriya, S., "A Time-Varying Sliding Surface for Fast and Robust Tracking Control of Second-Order Uncertain Systems," *Automatica*, Vol. 30, No. 5, 1994, pp. 899–904.

[13]Slotine, J. J. E., and Sastry, S. S., "Tracking Control of Nonlinear Systems Using Sliding Surfaces with Application to Robot Manipulators," *International Journal of Control*, Vol. 38, No. 2, 1983, pp. 465–492.

[14]Chen, C. T., *Linear System Theory and Design*, CBS College Publishing, New York, 1984, pp. 351–361.

[15]Sira-Ramirez, H., and Spurgeon, S. K., "On the Robust Design of Sliding Observers for Linear Systems," *Systems and Control Letters*, Vol. 23, No. 1, 1994, pp. 9–14.